




Publication Year	2021
Acceptance in OA @INAF	2023-02-21T13:47:23Z
Title	TURBULENCE PREDICTION: REPORT ON MODEL GEOMETRY
Authors	MASCIADRI, Elena; TURCHI, Alessio
Handle	http://hdl.handle.net/20.500.12386/33668

	
Project (Grant) Number:	824135
Project Acronym:	SOLARNET
Project title:	Integrating High Resolution Solar Physics

Document Details	
Document Title	TURBULENCE PREDICTION: REPORT ON MODEL GEOMETRY
Prepared by (Institution's Name):	INAF National Institute for Astrophysics
Work Package number & Title	WP7.3 Performance Characterization and Prediction
Deliverable number (if applicable)	D7.12
Document code (inserted by project office)	
File name (inserted by project office)	
Date uploaded (inserted by project office)	

AUTHORS/ CONTRIBUTORS LIST

Name	Function	Organization
Elena Masciadri	Researcher	INAF-OAA
Alessio Turchi	Researcher	INAF-OAA

APPROVAL CONTROL

Control	Name	Organization	Function	Date
Prepared	Alessio Turchi	INAF-OAA	Researcher	
Prepared	Elena Masciadri	INAF-OAA	Researcher-responsible of the activity	
Revised	Elena Masciadri	INAF-OAA		
Approved				
Authorized				

HISTORY OF DOCUMENT CHANGES

Issue	Date	Change Description
Version 1.0		Initial Issue

Table of Contents

1. Introduction.....	4
2. Model Geometry	4
2.1 Model geoemtry Roque de los Muchachos Observatory (ORM)	4
2.2 Model geometry Teide Observatory (TO)	10
2.3 Simulation scheme	14
3. Analysis of WF-WFS measurements taken at SST.....	15
4. Conclusions	19

List of Abbreviations

ORM	Roque de los Muchochos Observatory
TO*	Teide Observatory
GTC	Gran Telescope de Canarias
SST	Swedish Solar Telescope
ECMWF	European Centre for Medium Weather Forecast
OT	Optical Turbulence

*: In this document we use the acronym TO instead of OT for the Teide Observatory as OT is also the acronym of Optical Turbulence.

1. Introduction

The H2020 SOLARNET project includes a study to investigate the possibility to set-up systems for the forecast of the optical turbulence (OT) in the day-time regimes at the two sites of Roque de los Muchachos Observatory (ORM, La Palma) and Teide Observatory (TO, Tenerife), with a particular attention to the site that will be selected for the European Solar Telescope (EST). More precisely the study aims to upgrade to day-time conditions the method to forecast the OT (C_N^2 profiles and integrated astroclimatic parameters) that was developed by the INAF partner for night-time ground-based astronomy. The technique implies the use of a mesoscale model (Meso-Nh) [RF1, RF2, RF3, RF4]. Seeing measurements at the ORM and TO are presented in [RF5, RF6].

This document presents the global atmospheric model configuration. This includes the set-up of the orography and the sequence of initialisation. Besides, we analysed also measurements taken by the Stockholm University (SU) partner at the SST with the WF-WFS method in the past years in perspective of using such measurements as a reference to calibrate and/or validate forecasts. In [RF6] measurements taken with a SHABAR by the Instituto de Astrofísica de Canarias (IAC) partner during past years have been analysed with the same philosophy and goal. The analysis of WF-WFS measurements has to be seen as an integration of the [RF6]. We remind that measurements are relevant in this process as they represent the reference with respect to which we can provide an analysis of the forecasts.

2. Model geometry

In this section we present the results of the activity aiming to define the geometry of the model configuration to carry out the turbulence forecast. The first step is to define the configuration of the orography. On the basis of our past experience, we started with a configuration similar to that used for similar studies [RF1, RF2, RF3, RF4]. In Section 2.1 and 2.2 we describe the configuration respectively of the Roque del Los Muchachos Observatory (ORM) at La Palma and el Teide Observatory (TO) at Tenerife.

We use the Astro-meso-scale model Meso-Nh and the master version M542. We refer to [RF1] for the physics inside the model.

We use 62 vertical levels distributed following the law: the first grid point is 5 m, there is after a logarithm stretching of 20% up to the height of 3500 m above the ground. Above this threshold the grid size is of around 600 m up to 23.8 km above the ground. The model adjusts by itself the grid size in this part of the atmosphere assuming the number of grid-points and the distance between the threshold and the top of the atmosphere.

2.1 Model geometry: Roque de los Muchachos Observatory (ORM)

In Fig. 1 is shown the geographic map of the Canary Islands archipelago in which it is visible the La Palma isle (black arrow). The ORM Observatory is located on the summit of the central mountain region characterised by a *Caldera* having an arc shape. Fig. 2 shows the position of the mains telescopes located on the ORM in a satellite image extracted by Google Earth. The *Caldera* is characterised by very sharp slopes of the orography along its crater.

We centred our model on the position of the GTC (28.756611, -17.89188) and we used the grid-nesting techniques using three (configuration A) and four domains (configuration B) imbricated to achieve the maximum horizontal resolution in the region around the summit. The grid-nesting technique permits indeed

to use a set of imbricated domains extended on a smaller and smaller surface with the innermost domains characterised by the highest resolution. Table 1 reports the geometry of the configuration A and B. Configuration A is characterised by 3 domains and an innermost domain with a resolution of 0.5 km; configuration B is characterised by 4 domains and an innermost domain with a resolution of 0.1 km. Table 1 reports the number of grid pints, the extension of the surface and the horizontal resolution of the domains. Fig. 3, Fig. 4, Fig. 5 and Fig. 6 show the orography for domain 1, 2, 3 and 4 as seen by the mesoscale model Meso-Nh.

Fig. 7 and Fig. 8 show a zoom of the summit in which are visible the locations of a few telescopes of the ORM as seen by the model in configuration A and B.

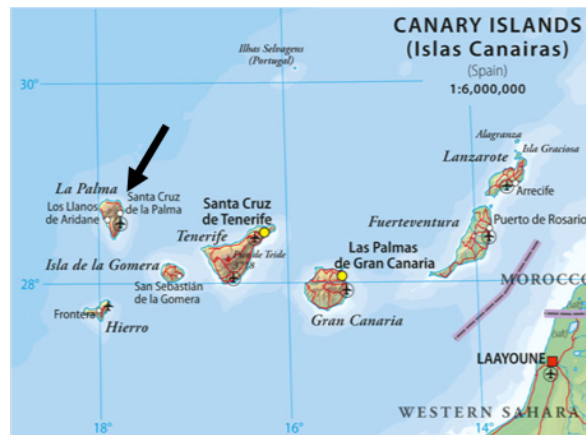


Fig. 1: Geographic map showing the Canary Islands archipelago. The black arrow indicates La Palma isle hosting the Roque de los Muchachos Observatory (ORM).



Fig. 2: Position of a few of the main telescopes belonging to the ORM located around the Caldera.

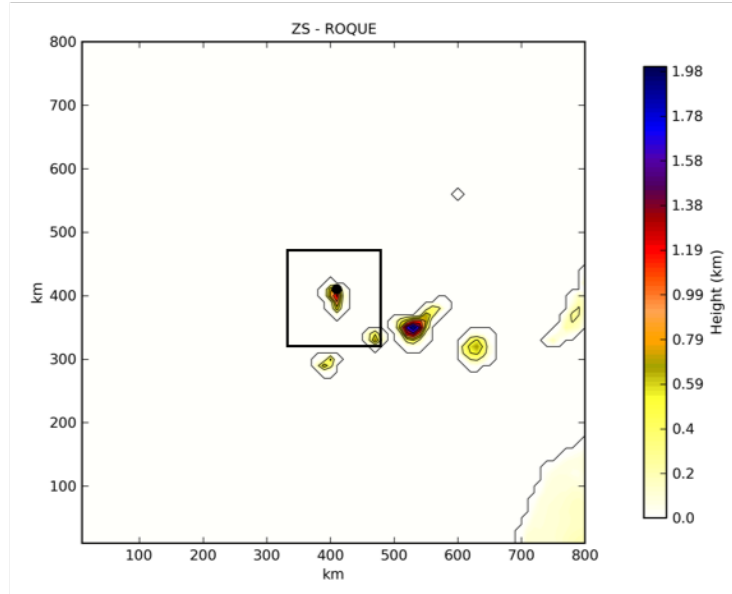


Fig. 3: La Palma Isle. The most external domain (DOM1) extended on 800 km x 800 km i.e. 80 x 80 grid points with a resolution of 10 km. The black square indicates the domain DOM2.

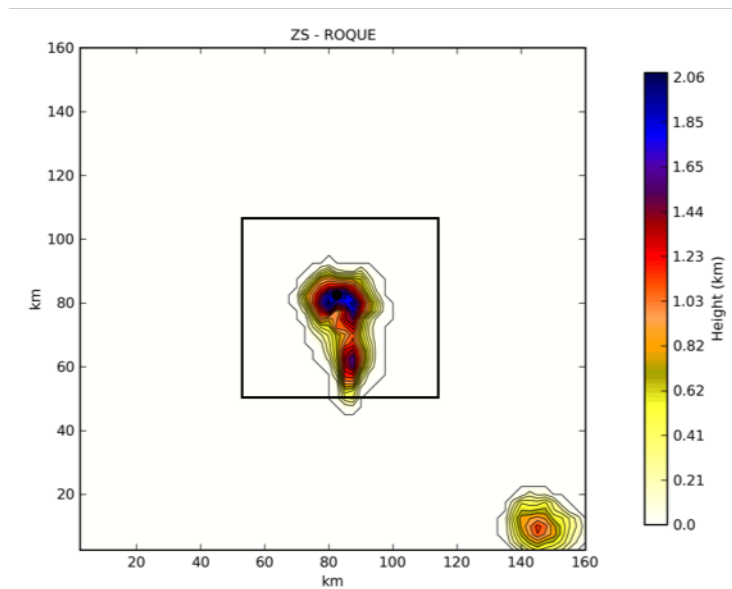


Fig. 4: La Palma Isle. The domain DOM2 extended on 160 km x 160 km i.e. 64 x 64 grid points with a resolution of 2.5 km. The black square indicates the most internal domain (DOM3).

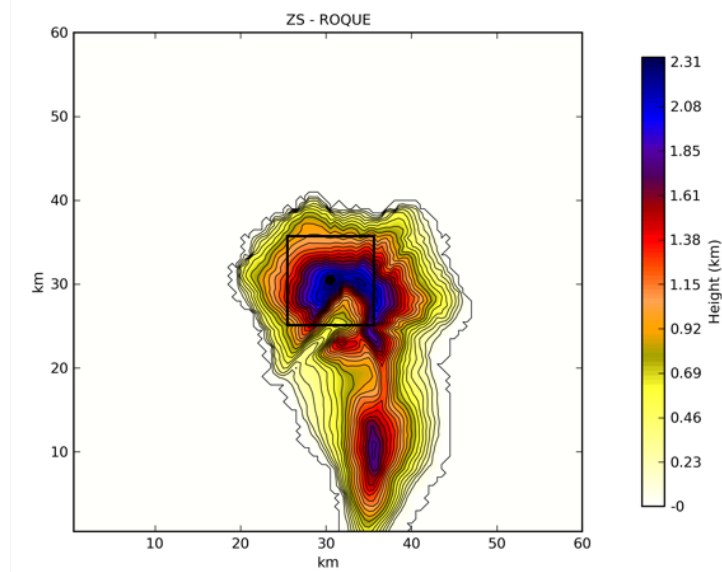


Fig. 5: La Palma Isle: The domain DOM3 extended on 60 km x 60 km i.e. 120 x 120 grid points with a resolution of 0.5 km.

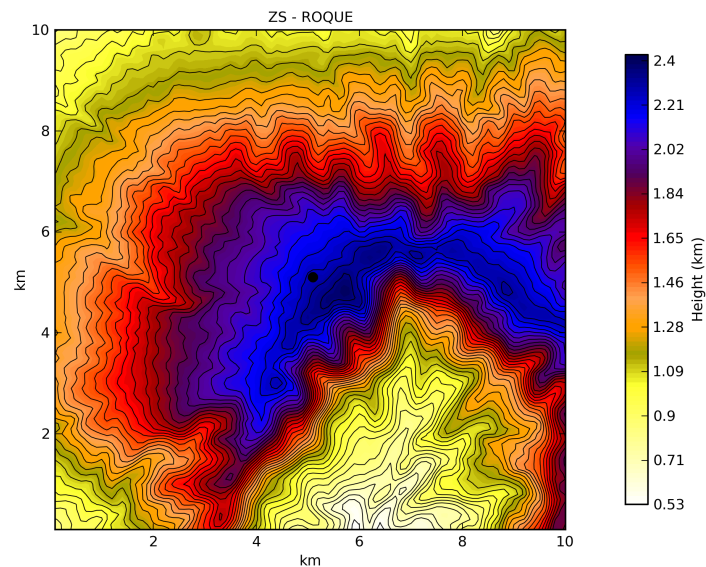


Fig. 6: La Palma Isle: The domain DOM4 extended on 10 km x 10 km i.e. 100 x 100 grid points with a resolution of 0.1 km.

Domain	Grid Points	Domain Size (km)	ΔX (km) – Hor. Resolution
Domain 1	80 x 80	800 km x 800 km	$\Delta X = 10$
Domain 2	64 x 64	160 km x 160 km	$\Delta X = 2.5$
Domain 3	120 x 120	60 km x 60 km	$\Delta X = 0.5$
Domain 4	100 x 100	10 km x 10 km	$\Delta X = 0.1$

Table. 1: Summary of the geometric characteristics of the model used in the grid-nesting configuration (see text). The same configuration has been used for La Palma and Tenerife.

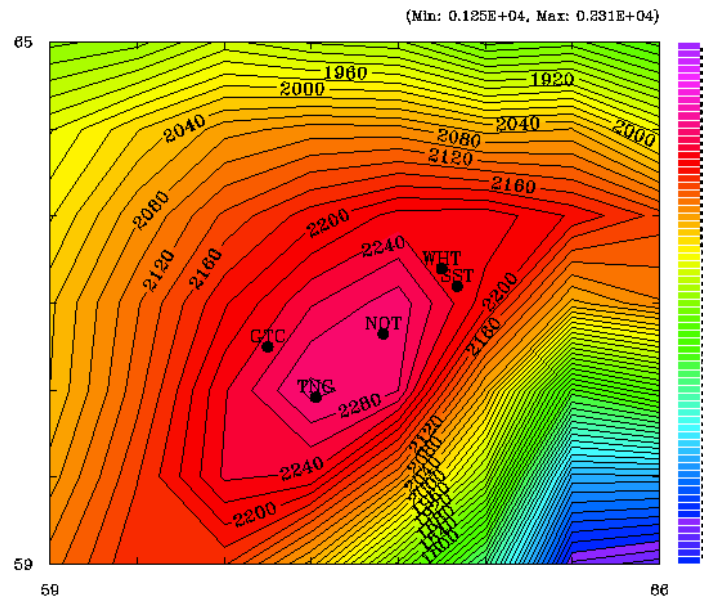


Fig. 7: ORM: Zoom of DOM3 (0.5 km resolution). Black dots indicate the position of a few of the main telescopes located on the summit. The SHABAR position is basically coincident with the SST.

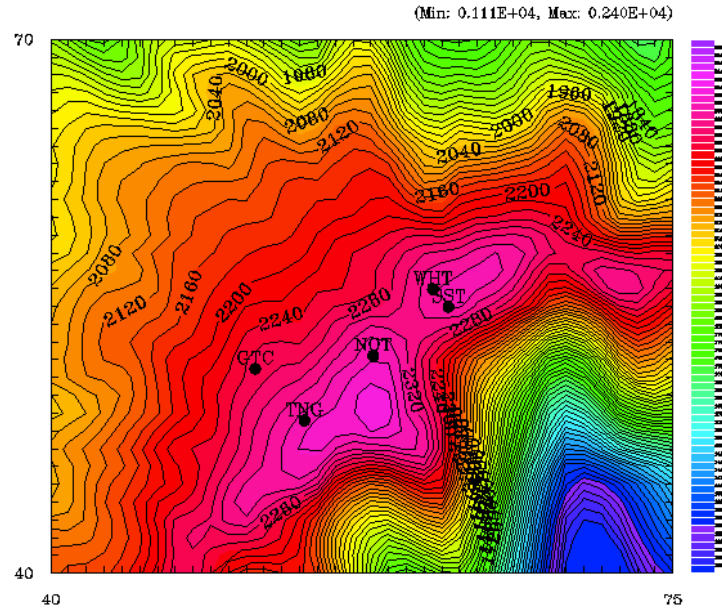


Fig. 8: ORM: Zoom of DOM4 (0.1 km resolution). Black dots indicate the position of a few of the main telescopes located on the summit. The SHABAR position is basically coincident with the SST.

Table 2 reports the difference between the heights reconstructed by the Meso-NH model and the real heights of different telescopes using the innermost domain having a resolution of 0.5 km (DOM3) and a resolution of 0.1 km (DOM4). A particular importance is the position of SST as in this location was placed the SHABAR [RF5] and are taken seeing measurements from the SU partner [RF6].

Telescopes	Real Height	ΔH (0.5 km)	ΔH (0.1 km)
SST	2365 m	73 m	54 m
TNG	2363 m	128 m	9 m
NOT	2384 m	77 m	25 m
WHT	2334 m	42 m	9 m
GTC	2270 m	32 m	8 m

Table. 2: Difference between the heights reconstructed by the Meso-NH model and the real height of different telescopes using the innermost domain having a resolution of 0.5 km (DOM3) and a resolution of 0.1 km (DOM4). The SHABAR was located basically at the same coordinates of SST during measurements (RF2).

2.2 Model geometry: Teide Observatory (TO)

Fig. 9 is the geographic map showing the Canary Islands archipelago. The black arrow indicates the Tenerife Isle. The Teide Observatory is located in the central mountain region. Fig. 10 shows some satellite images of Tenerife isle, the Teide Observatory and the location of a few telescopes.

We centred the model on the Vacuum Tower Telescope (VTT) having coordinates (28.302389 N, -16.51005 W). We used a grid-nesting with the same configuration indicated in Table 1. Fig. 11, Fig. 12, Fig. 13 and Fig. 14 show the orography for domain 1, 2, 3 and 4 as seen by the mesoscale model Meso-Nh.

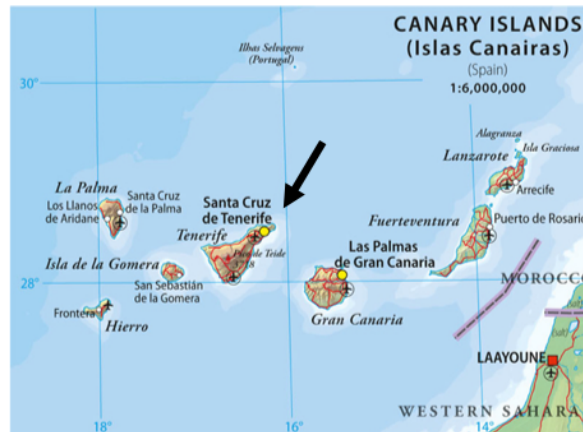


Fig. 9: Geographic map showing the Canary Islands archipelago. The black arrow indicates the Tenerife isle hosting the Teide Observatory (TO).

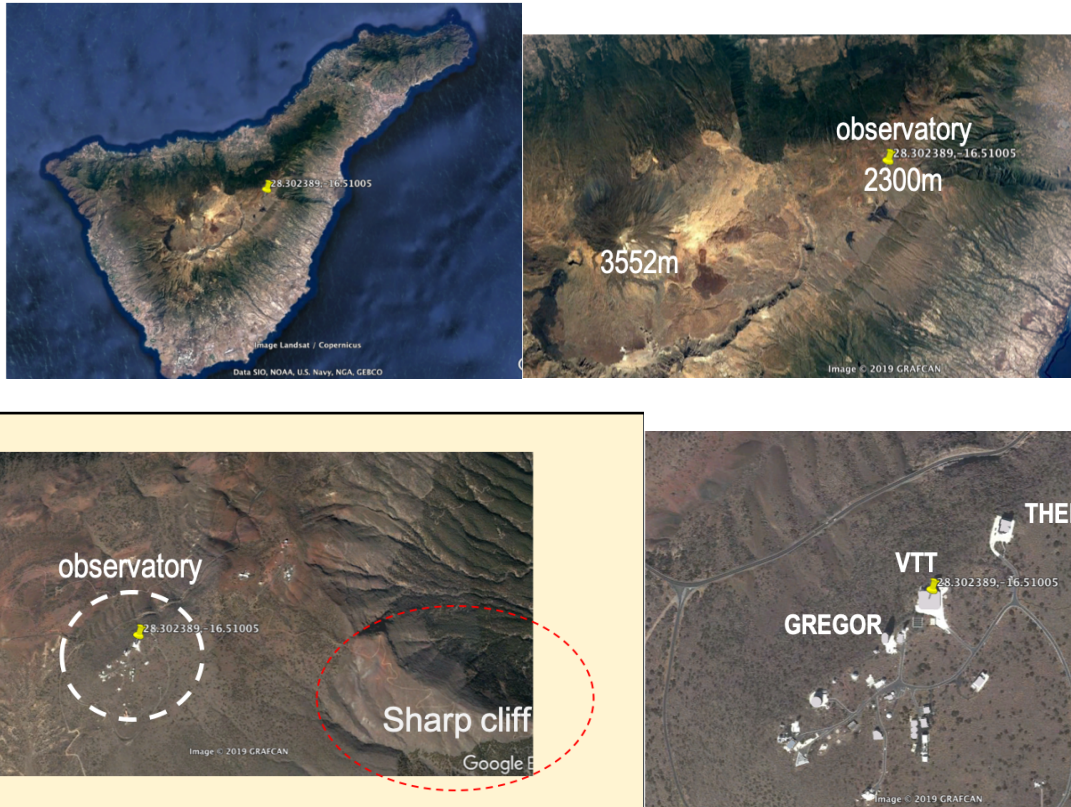


Fig. 10: Top-left: satellite view of the Tenerife Isle. Top-right: zoom of the region around the Teide Observatory in which it is visible a mountain on the West-side that is ~ 1 km higher than the TO summit. Bottom-left: a sharp cliff at the East with respect to the Teide Observatory. Bottom-right: position of the Vacuum Tower Telescope (VTT).

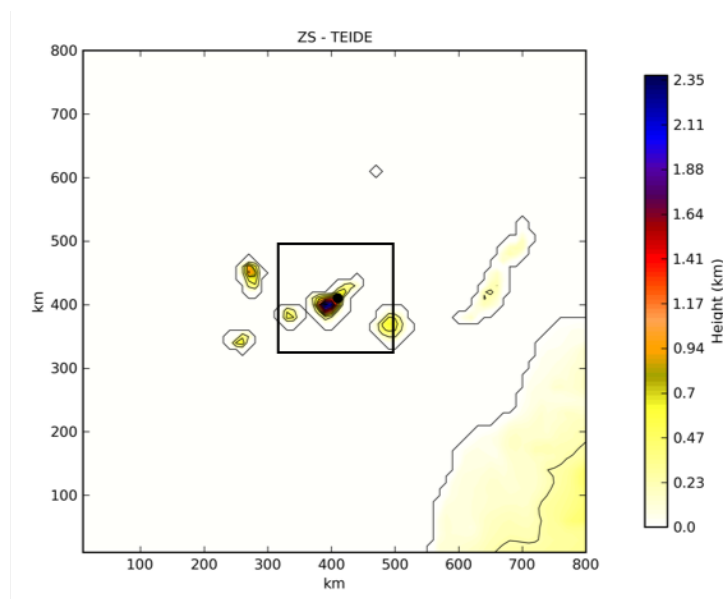


Fig. 11: Tenerife isle: The most external domain (DOM1) extended on 800 km x 800 km i.e. 80 x 80 grid points with a resolution of 10 km. The black square indicates the domain DOM2.

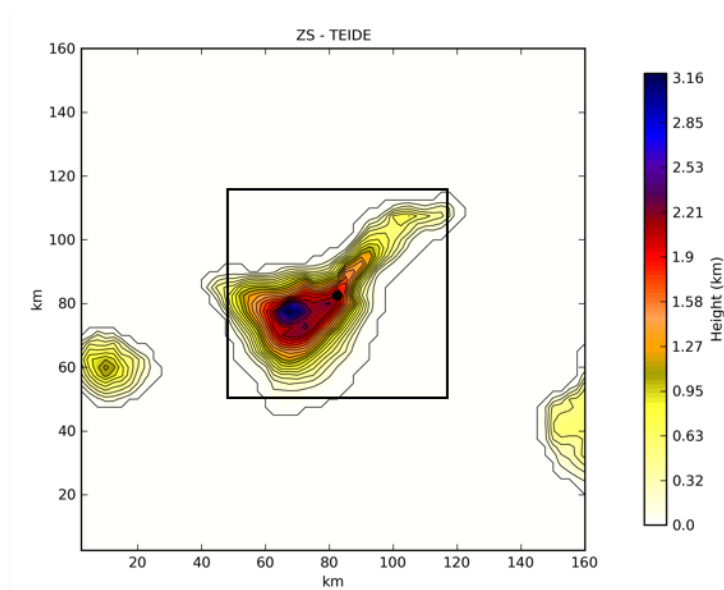


Fig. 12: Tenerife Isle: The domain DOM2 extended on 160 km x 160 km i.e. 64 x 64 grid points with a resolution of 2.5 km. The black square indicates the most internal domain (DOM3).

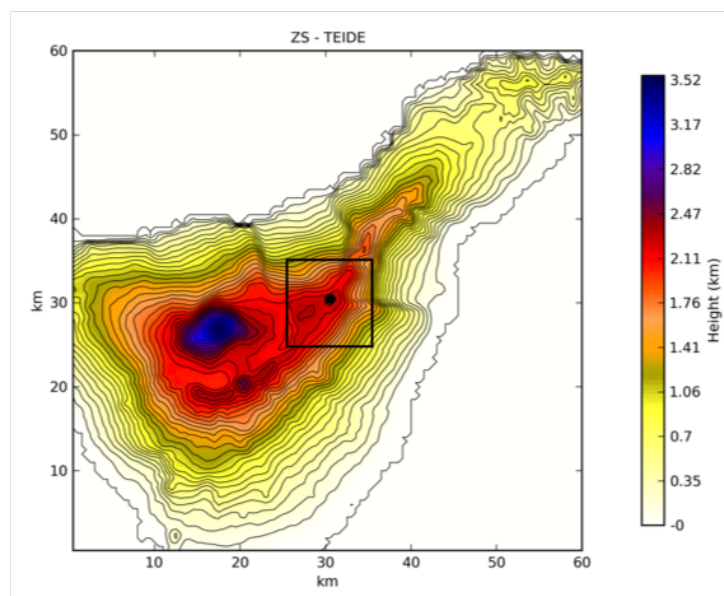


Fig. 13: Tenerife isle: The domain DOM3 extended on 60 km x 60 km i.e. 120 x 120 grid points with a resolution of 0.5 km.

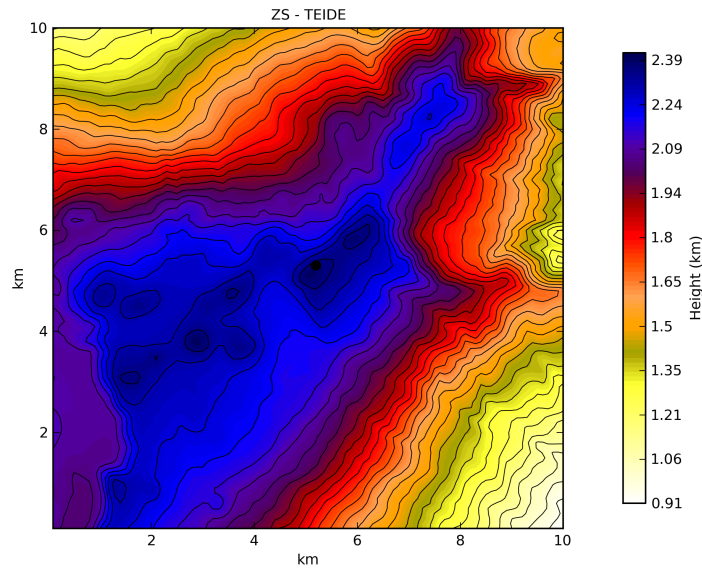


Fig. 14: Tenerife isle: The domain DOM4 extended on 10 km x 10 km i.e. 100 x 100 grid points with a resolution of 0.1 km.

Fig. 15 and Fig. 16 show a zoom of the summit of the TO in which are visible the locations of VTT and SHABAR as seen by the model in configuration A and B.

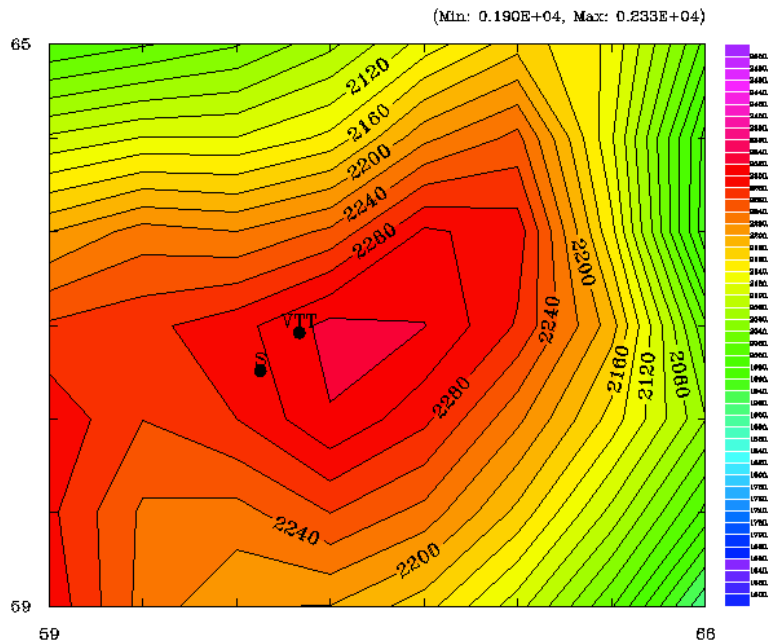


Fig. 15: TO: Zoom of DOM3 (0.5 km resolution). The black dot indicates the position of the VTT. The SHABAR position is indicated with ‘S’.

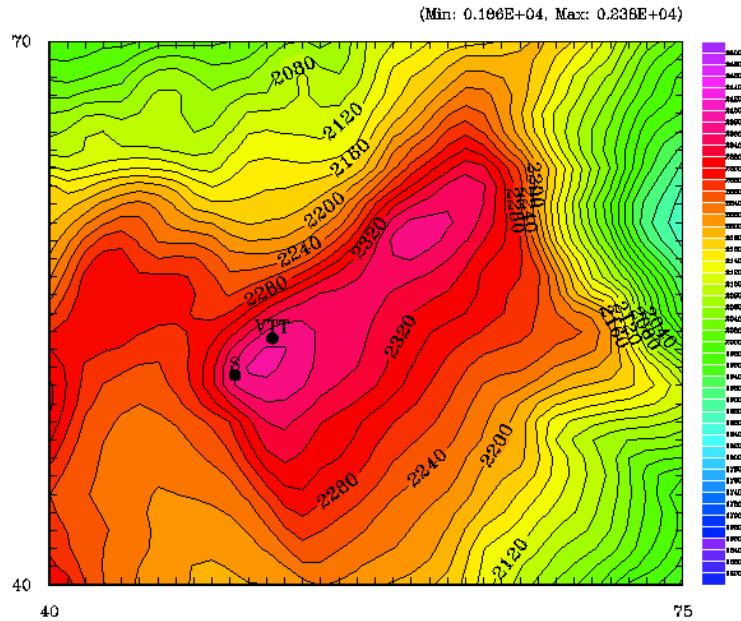


Fig. 16: TQ: Zoom of DOM4 (0.1 km resolution). The black dot indicates the position of the VTT. The SHABAR position is indicated with ‘S’.

Sites	Real Height	ΔH (0.5 km)	ΔH (0.1 km)
VVT	2387 m	107 m	4 m
SHABAR (‘S’)	2398 m	118 m	43 m

Table. 3: Difference between the height reconstructed by the Meso-Nh model and the real height of different sites using the innermost domain having a resolution of 0.5 km (DOM3) and the innermost domain having a resolution of 0.1 km (DOM4).

2.3 Simulation configuration scheme

The configuration of the model has been conceived to run couples of simulations/forecast (for the day and time period) as indicated in Fig. 17. We conceived a preliminary set-up without the aim to optimise the model performances but to use initialisation data already collected for the purposed of this project. Initialisation and forcing data for the numerical model come from the European Centre for Medium Weather Forecast (ECMWF). For the night time the simulation starts at 18:00 UT of the DAY (J-1) up to 15:00 UT of the DAY J. For the day period the simulation starts at 06:00 UT of the DAY (J-1) and finishes at 03:00 UT of the DAY J. Full line circles indicate the initialisation and forcing data. Dashed line circle are alternative solution for initialisation data that might be tested to refine eventually the configuration.

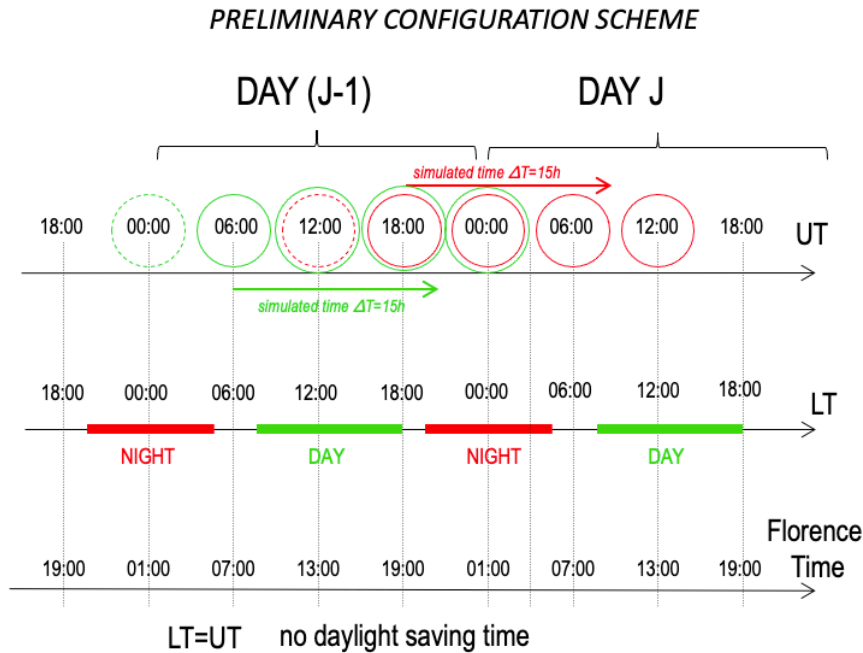


Fig. 17: Preliminary model scheme for the night and day time simulations.

3. Analysis of WF-WFS measurements taken at SST

Measurements of the OT are useful for the calibration and validation of the atmospheric model. Analysis of the measurements from SHABAR characterising the low part of the atmosphere has been presented in [RF6]. The SU partner is carrying on measurements of the OT during the day time using a WF-WFS mounted on the SST. Seeing measurements are performed using the so called WF-WFS technics [RF7]. Such a technique provides a stratification of the turbulence up to around 12 km from the ground as well as the seeing. Seeing measurements related to a rich statistical sample covering a few years has been provided to us by the SU partner. Measurements are in a raw format. Criteria of validity of measurements have been provided by Prof. Goran Scharmer (private communication).

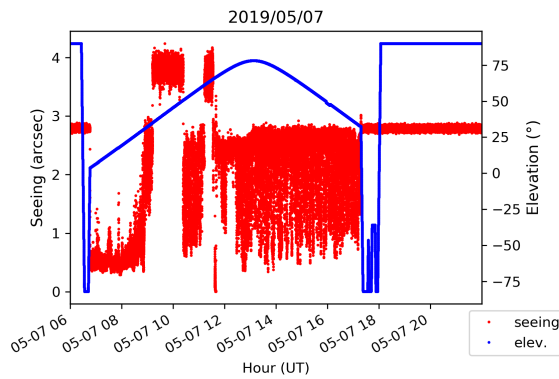


Fig. 18: Temporal evolution of the raw seeing during the night 2019/05/07. Red line is the raw seeing, the blue line represent the line of Sight (LoS) across the sky of the telescope. When the value of the blue line is smaller than 0 degrees or equal to 90 degrees (Y-axis on the right side) the telescope is not observing or it is approaching to a stop position.

As can be seen in Fig. 18 showing an example of raw seeing measured by the WF-WFS, it is evident a saturated level of the seeing at around 2.5”-2.6” between 12 and 17 UT. The criteria for measurements validity indicates that **(1)** seeing values to be retained are included in the temporal window within which the telescope move across the sky (Fig. 18: elevation displayed with blue line). When the blue line value is smaller than 0 or equal to 90 degrees the seeing values are not valid as the telescope is simply not observing or it is approaching to a stop position. Seeing values different from zero correspondent to these intervals are spurious values; **(2)** values above a threshold of around 2.5”-2.6” inside the temporal window in which the telescope is observing and clearly tracking the sun on sky have to be rejected as not valid.

In the example we have just shown, the valid seeing values are reported in Fig. 19.

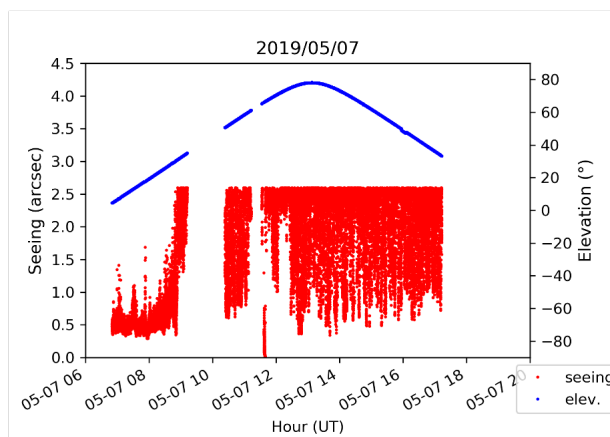


Fig. 19: As Fig.18 but with applied criteria imposed on the seeing validity (see text).

We finally applied a moving average of 1h to provide readable measurements (see Fig. 20).

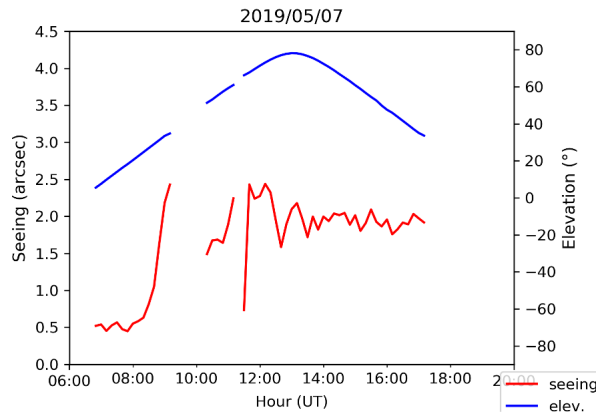


Fig. 20: As Fig.19 but with moving average of 1h.

In Fig. 21 are shown a few cases in which is visible the seeing saturation at 2.5” within the temporal window in which the telescope is observing. It is also evident as sometime the seeing assumes values larger than 2.5” that based on the criteria of measurements validity are discarded.

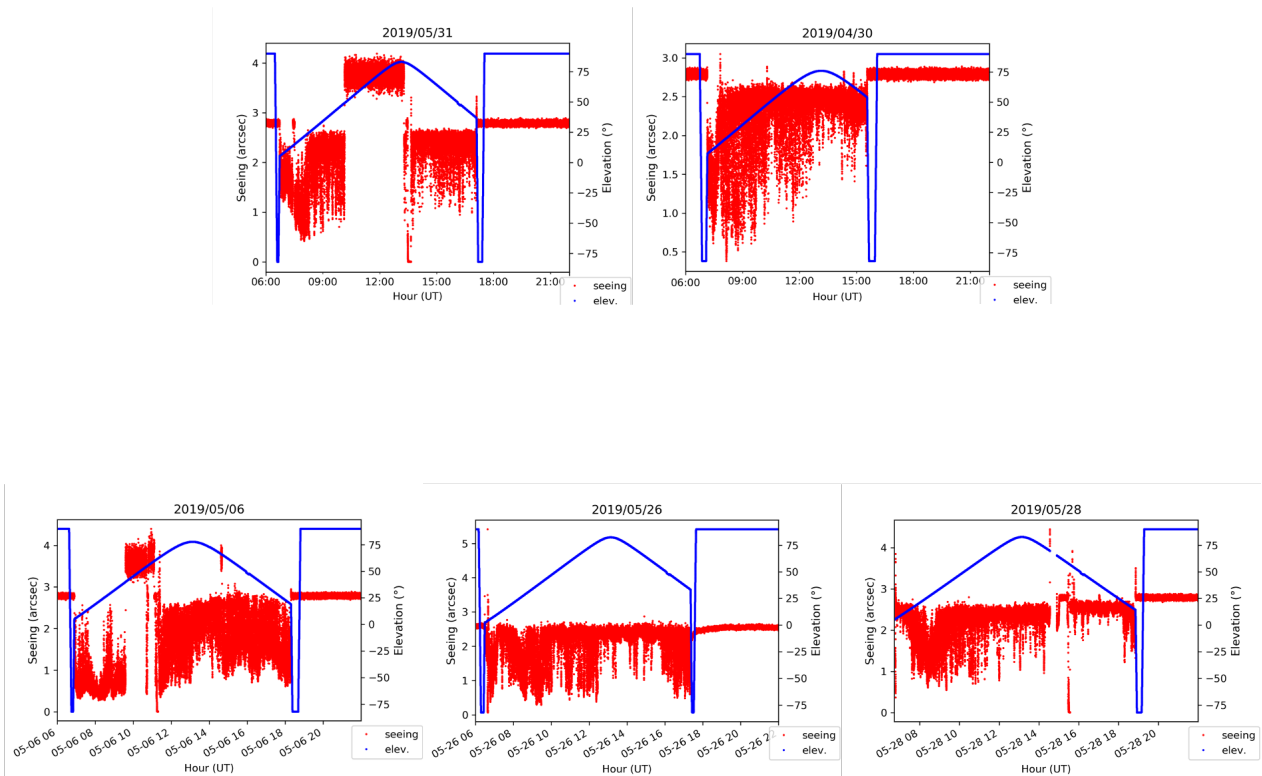


Fig. 21: A few examples of raw seeing measurements belonging to the database.

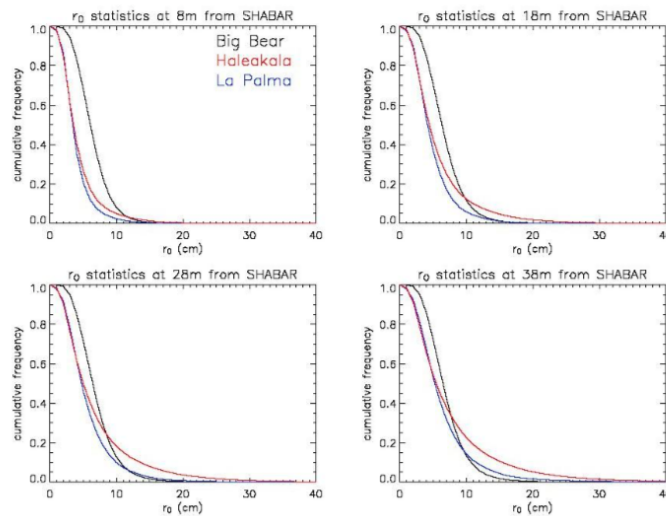


Fig. 22: Extracted from [RF8]. Cumulative distribution of r_0 at different heights above the ground.

We observe that the fact that there is a saturation level at 2.5” means that the measurement method does not cover the whole range of the turbulence energy and part of the turbulence energy spectrum is not detected by the method. This fact is very unusual since results belonging to the literature (see for example Fig. 22 from [RF8]) indicate a continuum range of values of r_0 from 0 to around 30 cm - 40 cm without any thresholds. Fig. 22 indicates $r_0(h)$ values at four different heights. That means the r_0 calculated between h and the end of the atmosphere. Measurements done with the WF-WFS correspond to the height of the STT. We do not know the exact height, but it is presumably between 8 m and 18 m. Looking at the panels on the top of Fig. 22 we see that $r_0(h)$ at La Palma does not present an interruption in continuity on the r_0 values.

We note moreover that, if we assume that the seeing $\leq 2.5''$, that means $r_0 \geq 3.9$ cm. However, we observe (Fig. 23 from [RF9]) that the median value of r_0 measured at La Palma by another team in the past at around 10 m above the ground is of the order of 3.5 cm. It seems therefore highly probable that some filtering effects are present in the measurements we are treating and a part of the turbulent spectrum is missing, as it is difficult to figure out that a sample of measurements in which $r_0 \geq 3.9$ cm provides a median value of $r_0 = 3.5$ cm. That indicates that many r_0 smaller than 3.9 cm are in reality not detected or not considered in the total energetic budget.

We suspect therefore that the method developed by the SU partner is not reliable to provide an absolute estimate of the total seeing, from the ground up to the weakest turbulent layers in the high altitude. We intend to better investigate on this point in the future with the SU partner. We point out that this fact represents a limitation in all contexts in which an absolute estimate of the seeing is important as is our case.

In [RF7] conclusion is declared that the method proposed allows good seeing measurements when $r_0 > 7.5$ cm for the ground layer. This seems to go in the direction of our interpretation of data.

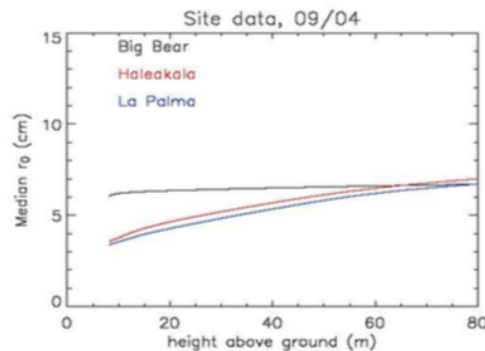


Fig. 23: Extracted from [RF9]. Median r_0 at different heights above the ground for La Palma.

4. Conclusions

This document describes the geometry of the set-up given by the orographic and the atmospheric models that will be used to study the turbulence prediction with the mesoscale model (Astro-Meso-Nh) as in the aim of the SOLARNET WP7.3. The orography of the Roque de los Muchachos Observatory at La Palma, and of the Teide Observatory at Tenerife, Canary Islands, which are the two perspectives sites for the European Solar Telescope (EST), have been considered for the model configuration, as well as a preliminary model running scheme for night- and day-time simulations.

Besides, we integrate [RF6] (that treats SHABAR measurements done by IAC partner) with the analysis of WF-WFS measurements taken by SU partner. Both observations (by SHABAR and WF-WFS) are extended on a relatively rich statistical sample of measurements and for this reason useful for our application. Unfortunately, at present we remark a lack of estimate of the total absolute seeing values done with the WF-WFS observations that makes the study of the OT forecast much more complex than what we had envisaged.

The document D7.10 from the SU partner on the turbulence profile comparison should be available at T0+30 months. For that time measurements of the OT stratification should be available.

References

Documents	Title
RF1	Masciadri, E. et al., 2020, MNRAS, 492, 140
RF2	Masciadri, E. et al., 2017, MNRAS, 466, 520
RF3	Turchi, A. et al., 2019, MNRAS, 482, 206
RF4	Turchi, A. et al., 2020, MNRAS, 497, 4910
RF5	D70.8: Results of the site testing campaign at ORM and OT – May 2017 (312495 - FP7 SOLARNET)
RF6	D7.11: Turbulence prediction: report on available measurements – December 2019 (824135 - H2020 SOLARNET)
RF7	Scharmer, G.B. & van Werkhoven, T.I.M, 2010, A&A, 513, A25
RF8	Socas-Navarro, H. et al. 2005, PASP, 117, 1296
RF9	Hill, F. et al., 2006, SPIE 62671T, doi: 10.1117/12.673677